347-361 (2013).

20. Reavie, L., Buckley, S.M., Loizou, E., Takeishi, S., Aranda-Orgilles, B., Ndiaye-Lobry, D., Abdel-Wahab, O., Ibrahim, S., Nakayama, K.I., Aifantis, I. Regulation of c-Myc ubiquitination controls chronic myelogenous leukemia initiation and progression. *Cancer Cell* **23**, 362-375 (2013).

21. Furutachi, S., Matsumoto, A., Nakayama, K.I., Gotoh, Y. p57 controls adult neural stem cell quiescence and modulates the pace of lifelong neurogenesis. *EMBO J.* in press. (2013).

2. 学会発表

1. 中山敬一: ヒトプロテオーム絶対定量プロジェクト：網羅的ターゲットプロテオミクスの開発と応用. 基生研研究会「モデル生物・非モデル生物のプロテオミクスが拓く生物学」. (招待講演) 岡崎.5/14 (2012).

2. Nakayama, K.I.: Comprehensive profiling of cancer metabolism by the next generation proteomics. **10th Stem Cell Research Symposium**. (Invited speaker) Awaji.5/31 (2012).

3. 中山敬一: 次世代プロテオミクスが拓く医学研究の新地平：もうウェスタンブロッティングは要らない？！. 第 55 回日本腎臓学会学術総会. (招待講演) 横浜.6/1 (2012).

4. 中山敬一: 次世代プロテオミクスが拓く生命科学研究の新地平：もうウェスタンブロッティングは要らない？！. 疾患関連創薬バイオマーカー探索研究. (招待講演) 東京.6/21 (2012).

5. 中山敬一: 次世代プロテオミクスが拓く生命科学研究の新地平：もうウェスタンブロッティングは要らない？！. 第 22 回日本サイトメトリー学会学術集会. (招聘講演) 豊中.6/29 (2012).

6. 幡野敦, 松本雅記, 中山敬一: 定量的リン酸化プロテオミクスによる Calcineurin の網羅的基質探索. 第 10 回日本プロテオーム学会. 東京.7/26 (2012).

7. 松本雅記: 定量プロテオミクスのための試料調製. 第 10 回日本プロテオーム学会. (教育講演) 東京.7/26 (2012).

8. 中山敬一, 松本雅記, 押川清孝, 松崎芙美子: ヒトプロテオーム絶対定量プロジェクト：網羅的ターゲットプロテオミクスの開発と応用. 第 10 回日本プロテオーム学会. (シンポジウム) 東京.7/26 (2012).

9. 中山敬一: プロテオームと疾患研究. ヒトプロテオゲノミクスの現状とロードマップによる推進：エピゲノムとプロテオームの統合によるヒトの生命と病気の解明. (シンポジウム) 東京.7/28 (2012).

10. Nakayama, K.I.: Comprehensive and unbiased identification of substrates for ubiquitin ligases by differential proteomics analysis. **HUPO 2012 11th World Congress**. (Invited speaker) Boston, MA.9/12 (2012).

11. 中山敬一: G0 期維持機構の解

明：癌幹細胞を撲滅できるか？. 第 71 回日本癌学会学術総会. (シンポジウム) 札幌.9/19 (2012).

12. 松本雅記, 松崎芙美子, 高見知代, 小山田浩二, 中山敬一: 情報基盤プロテオミクスによるヒトプロテオームの絶対定量. 第 5 回定量生物学の会年会. (招待講演) 東京.11/24 (2012).

13. 喜多泰之, 西山正章, 中山敬一: クロマチンリモデリングタンパク質 CHD7 の新規スプライシングバリアントの発見とその機能解析. 第 35 回日本分子生物学会年会. 福岡.12/11 (2012).

14. 渡邉心也, 杉本のぞみ, 松本雅記, 中山敬一, 藤田雅俊: プロテオミクスアプローチを用いた新規 GRWD1 結合タンパク質の網羅的同定による GRWD1 の機能解明. 第 35 回日本分子生物学会年会. 福岡.12/11 (2012).

15. 中山敬一: 正常幹細胞と癌幹細胞における G0 期維持機構："G0 期追出し療法"による癌根治の可能性. 第 35 回日本分子生物学会年会. (ワークショップ) 福岡.12/11 (2012).

16. 橋本寛, 松崎芙美子, 細田將太郎, 大西隆史, 中山敬一, 白根道子: Protrudin が関与する遺伝性痙性対麻痺の病態メカニズム. 第 35 回日本分子生物学会年会. 福岡.12/12 (2012).

17. 細田將太郎, 清水誠之, 石谷太, 中山敬一, 白根道子: 新規 FKBP38 結合タンパク質 ANKMY2 はソニックヘッジホッグシグナル伝達を制御する. 第 35 回日本分子生物学会年会. (ワークショップ) 福岡.12/13 (2012).

18. 磯下理恵子, 小野山一郎, 鈴木淳史, 松本有樹修, 冨田謙吾, 片桐秀樹, 尾池雄一, 中山啓子, 中山敬一: Fbxw7 はマウスの肝臓において脂質代謝及び細胞分化決定を制御する. 第 35 回日本分子生物学会年会. 福岡.12/13 (2012).

19. 諸石寿朗, 西山正章, 岩井一宏, 中山敬一: ユビキチンリガーゼ FBXL5 による鉄代謝制御と肝がん. 第 35 回日本分子生物学会年会. 福岡.12/13 (2012).

20. 中津海洋一, 松本雅記, 小山田浩二, 中山敬一: mTOR と転写をつなぐ新規分子 FOXK1 の発見とがん進展における促進作用. 第 35 回日本分子生物学会年会. (ワークショップ) 福岡.12/13 (2012).

21. 足達俊吾, 穂本真佐江, 田中利好, 日置雄策, 村上裕, 菅裕明, 松本雅記, 中山敬一, 堀本勝久, 家村俊一郎, 夏目徹: 質量分析計による RNA 制御因子の同定法の開発とその応用. 第 35 回日本分子生物学会年会. (ワークショップ) 福岡.12/13 (2012).

22. 大西隆史, 橋本寛, 細田將太郎, 中山敬一, 白根道子: 神経特異的な protrudin 新規アイソフォームの発現機能解析. 第 35 回日本分子生物学会年会. 福岡.12/14 (2012).

23. 平野有沙, 恒松良佑, 松本雅記, 尾山大明, 秦裕子, ランジャコーンシリパンダーリン, 中山敬一, 深田

吉孝: F-box タンパク質によるユビキチン化を介した CRY タンパク質の安定性制御. **第 35 回日本分子生物学会年会**. (ワークショップ) 福岡.12/14 (2012).

24. 沖田康孝, 松本有樹修, 弓本佳苗, 磯下理恵子, 中山敬一: Fbxw7 の発現抑制は iPS 細胞形成を促進する. **第 35 回日本分子生物学会年会**. 福岡.12/14 (2012).

25. 山内隆好, 西山正章, 諸石寿朗, 弓本佳苗, 押川清孝, 中山敬一: MDM2 による RNA ヘリカーゼ DDX24 の非分解的制御機構の解明. **第 35 回日本分子生物学会年会**. 福岡.12/14 (2012).

26. 弓本佳苗, 秋吉清百合, 小野山一郎, 森正樹, 三森功士, 中山敬一: 宿主 Fbxw7 が癌転移を抑制する. **第 35 回日本分子生物学会年会**. (ワークショップ) 福岡.12/14 (2012).

27. 武石昭一郎, 松本有樹修, 小野山一郎, 仲一仁, 平尾敦, 中山敬一: Fbxw7 阻害は静止期を破綻させることにより白血病幹細胞を根絶する. **第 35 回日本分子生物学会年会**. 福岡.12/14 (2012).

28. 諸石寿朗, 西山正章, 山内隆好, 武田有紀子, 岩井一宏, 中山敬一: 生体における鉄代謝制御の中心をなす FBXL5-IRP2 系の発見. **第 85 回日本生化学会大会**. (シンポジウム) 福岡.12/15 (2012).

29. Matsumoto, M., Matsuzaki, F., Oshikawa, K., Oyamada, K., Goshima, N., Natsume, T., Nakayama, K.I.: Accurate and absolute quantification of human proteome by large-scale targeted proteomics. **第 85 回日本生化学会大会**. (シンポジウム) 福岡.12/15 (2012).

30. Kuroda, S., Yugi, K., Kubota, H., Soga, T., Matsumoto, M., Nakayama, K.I.: Unbiased identification of global network for signaling and metabolism from trans-omic data. **第 85 回日本生化学会大会**. (シンポジウム) 福岡.12/15 (2012).

31. 平野有沙, 恒松良佑, 松本雅記, 尾山大明, 秦裕子, ランジャコーンシリパンダーリン, 中山敬一, 深田吉孝: 時計タンパク質 CRY の安定化を担う新規ユビキチンリガーゼの同定. **第 85 回日本生化学会大会**. (口頭発表) 福岡.12/16 (2012).

32. 中山敬一, 西山正章, 諸石寿朗: ユビキチン化による鉄代謝制御機構とその破綻. **第 85 回日本生化学会大会**. (シンポジウム) 福岡.12/16 (2012).

33. 中山敬一: ユビキチンシステムの網羅的解析基盤の創出. **戦略的創造研究推進事業 (CREST)「生命システムの動作原理と基盤技術」研究領域・平成 24 年度公開シンポジウム**. (シンポジウム) 東京.2/25 (2013).

34. Yamauchi, T., Nishiyama, M., Moroishi, T., Yumimoto, K., Nakayama, K.I.: MDM2 mediates nonproteolytic polyubiquitylation of the DEAD-box RNA helicase DDX24 to regulate pre-rRNA processing. **Post-GCOE Symposium & Retreat on Cell-fate**

decision: Function and dysfunction in homeostasis. (Oral) Singapore.3/4 (2013).

35. Takeishi, S., Matsumoto, A., Onoyama, I., Naka, K., Hirao, A., Nakayama, K.I.: Ablation of Fbxw7 eliminates leukemia-initiating cells by preventing quiesence. **Post-GCOE Symposium & Retreat on Cell-fate decision: Function and dysfunction in homeostasis**. (Oral) Singapore.3/4 (2013).

36. Yamamura, S., Yumimoto, K., Nakayama, K.I.: Fbxw7-dependent ubiquitylation mediates the degradation of SOX9. **Post-GCOE Symposium & Retreat on Cell-fate decision: Function and dysfunction in homeostasis**. (Oral) Singapore.3/5 (2013).

H. 知的財産権の出願・登録状況

1. 特許取得
   該当なし

2. 実用新案登録
   該当なし

3. その他
   該当なし

厚生労働科学補助金（創薬基盤推進研究事業）分担研究報告

「疾患関連創薬バイオマーカー探索研究」

	氏名	所属	職名
分担研究者	黒光貞夫、鞍馬岳吏	アステラス製薬	室長、主管研究員

研究要旨

肝細胞癌で有用性の高い（発現の高特異性・高頻度、癌細胞増殖・生存に関わる機能を有する）創薬バイオマーカー探索を目的に、国立がんセンターで取得された肝細胞癌症例50例における腫瘍組織と非腫瘍組織のエキソンアレイデータを用いて、腫瘍組織で選択的な発現を示す分泌因子に着目し、その機能解析を実施した。また、スキルス胃癌での同様な創薬バイオマーカー探索を目的に、胃癌細胞株のRNAディープシークエンシング解析より融合変異遺伝子の抽出とその機能解析を実施した。

A. 研究目的

肝細胞癌は本邦では悪性腫瘍死の第4位を占める。肝細胞癌の5年生存率は40%程度と不良である。また、スキルス胃癌は若年者に多く、進行が早く早期発見が困難な癌である。両癌ともに治療成績の向上を目指した診断法と治療法の早期開発が望まれる。

高頻度に腫瘍組織特異的に発現し、癌細胞の増殖・生存に関わる可能性のある遺伝子は診断のためのバイオマーカー候補であると同時に、治療標的候補となる可能性がある。

本研究では、国立がんセンターで手術を受けた肝細胞癌症例の手術検体のエキソンアレイデータを用いて、腫瘍組織で選択的な発現を示す遺伝子を抽出、その機能解析を行って、新たな診断且つ治療に有用な標的分子の同定を目的とする。具体的な例として肝細胞癌においては、11q13.3領域増幅により発現亢進した分泌因子FGF19がオンコジェニックドライバーとなっている例が報告されている（Cancer Cell 2011, 19, 347-358）。本年度は肝細胞癌50例における腫瘍組織と非腫瘍組織のエキソンアレイデータを用いて、特に腫瘍組織で選択的な発現を示す分泌因子に着目し、その機能解析を行った。

一方、本邦での非小細胞肺癌におけるEML4-ALK融合変異キナーゼの発見以来、特定癌種での診断マーカー且つ治療標的として、癌細胞増殖・生存に関わる変異キナーゼの探索が盛んになってきた。本研究では、肝細胞癌症例の手術検体や胃癌細胞株のエキソンアレイ解析、ディープシークエンシ

ング解析により見出した変異遺伝子の機能解析を行い、新たな診断且つ治療に有用な標的分子の同定を目的とする。

前年度までキナーゼに着目した癌原性を示す変異遺伝子の探索を行ってきたが、本年度は胃癌細胞株の RNA ディープシークエンシング解析よりみいだした非キナーゼ融合変異遺伝子の機能解析を実施した。

B. 研究方法

国立がんセンターで取得された肝細胞癌症例 50 例における腫瘍組織と非腫瘍組織のエキソンアレイデータをアステラス製薬において解析し、腫瘍組織選択的に発現する分泌因子であること、高発現する肝癌細胞株が入手可能であること、正常組織での発現が認められない／あるいは限定的であることを指標に標的妥当性検証に進める候補分子を選抜した。qPCR で発現を確認した肝癌細胞株を用い、siRNA によるノックダウン試験を行い増殖への寄与を検討した。

一方、スキルス胃がん細胞 7 株、HSC39, HSC43, HSC44, HSC45, HSC58, HSC59, HSC60 の RNA のディープシークエンシング解析データを国立がん研究センター研究所にて取得した。アステラス製薬において融合遺伝子候補を抽出し、本遺伝子を発現する細胞株で腫瘍増殖ドライバー変異としての可能性を検討した。

（倫理面への配慮）

国立がんセンターの倫理委員会による審査で承認された方法で採取保管され、検体の個人情報が漏出することが無いように匿名化が厳重に行われるように配慮したがん患者の手術検体を用いた。また、本共同研究は国立がんセンターの倫理委員会およびアステラス製薬の倫理委員会において審査・承認された。

C. 研究結果

肝細胞癌症例 50 例のエキソンアレイデータより、B. に記載の指標で標的妥当性検証に進める分泌因子 6 個を選抜した（表１）。

肝癌細胞 16 株における各分泌因子の発現を qPCR で確認し、高発現する株を特定した。これら細胞株を用い、siRNA による発現抑制の増殖への寄与を検討した。

その結果、いずれの分泌因子のノックダウンも、当該分子を発現する肝癌細胞株において顕著な増殖抑制は認められなかった。

スキルス胃癌細胞株の RNA ディープシークエンシング解析データから 3 個の非キナーゼ融合変異遺伝子候補を抽出した。RT-PCR にて融合遺伝子の発現が確認された細胞株を用い、腫瘍増殖ドライバー変異の可能性を検討するため、siRNA によるノックダウン試験を実施した。

図 3 に示す通り、RT-PCR により融合変異遺伝子 X の増幅が HSC39 細胞で確認された。一方、HSC58 細胞では増幅が観察されなかった。

図1に示すように融合変異遺伝子Xの3'側パートナー遺伝子Zに対するsiRNAを作製した。siRNA Z-1、Z-2は融合変異遺伝子X及び野生型遺伝子Z両方を認識し、その発現を抑制する。一方、siRNA Z-4、Z-5は野生型遺伝子Zの発現のみ抑制するように設計、作製した。

これらsiRNAを用いてノックダウン試験を行った結果、siRNA Z-1、Z-2はいずれも当該融合変異遺伝子を発現するHSC39の細胞増殖を強く抑制した（図2）。一方、野生型遺伝子Zのみを認識するsiRNA Z-4、Z-5はHSC39の細胞増殖抑制作用をほとんど示さなかった。HSC58細胞においてはいずれのsiRNAともに細胞増殖への顕著な作用を示さなかった。

他2融合変異遺伝子のうちの一つである融合変異遺伝子DIS3L（1-305残基）-CHAF1A（892-956残基）についてはこれを発現するHSC39において、siRNAによるDIS3Lの発現抑制は細胞増殖抑制作用を示さなかった。また、他方の融合変異遺伝子PHRF（1-1621残基）-PTDSS2（62-487残基）についてはこれを発現するHSC44において、siRNAによるPTDSS2及びPHRFの発現抑制は顕著な細胞増殖抑制作用を示さなかった。

D. 考察

スキルス胃癌細胞株のRNAディープシークエンシング解析データより見出した非キナーゼ融合変異遺伝子候補Xは、内在発現を示すHSC39での機能検証実験より、当該細胞において腫瘍増殖ドライバーとして機能する可能性が示唆された。

一方、融合変異遺伝子DIS3L-CHAF1A、PHRF-PTDSS2及び肝細胞癌手術検体のエキソンアレイより見いだした分泌因子A-Fに関しては、内在発現を示す細胞株での機能検証実験結果より、治療標的候補としての可能性がないと判断し、更なる検討を実施しないこととした。

E. 結論

スキルス胃癌細胞株において新規の非キナーゼ融合変異遺伝子候補Xを見出した。治療標的候補として更に全長のクローニング、腫瘍特異的な発現、癌化能の有無について検討を進める。

F. 健康危険情報

特になし

G. 研究発表

特になし

H. 知的財産権の出願・登録状況（予定を含む）

特になし

表1. 肝細胞癌手術検体のエキソンアレイデータにより選抜した分泌因子

	発現陽性数			機能検証を実施した細胞株
	HCC 手術検体 (n=50)		肝癌細胞 (23株)	
	腫瘍組織	非腫瘍組織		
分泌因子A	17	0	19	SK-HEP-1, HuH-7, HuH-28, HuH-6 clone 5
分泌因子B	9	0	8	HuH-28, SNU-398
分泌因子C	9	0	18	HLF, SNU-387, HuH-28
分泌因子D	3	0	9	HuH-6 clone 5
分泌因子E	21	0	15	SNU-387, SK-HEP-1, HUH-6 clone 5, Hep G2
分泌因子F	13	0	2	Hep G2, HUH-6 clone 5, HuH-7

図1. 融合変異遺伝子 X の推定構造と
qPCR primer、siRNA の設計位置

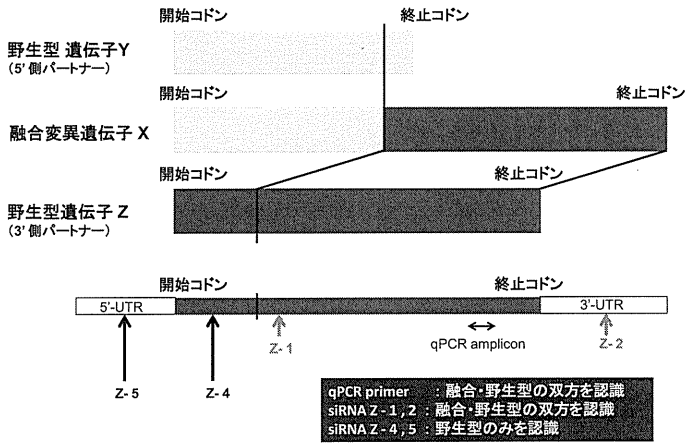

図2. HSC39 の増殖における融合変異遺伝子 X の寄与

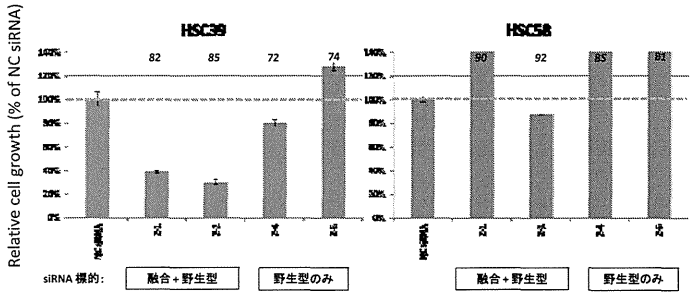

・図中の数値は siRNA による mRNA 発現抑制率を示す。
・relative cell growthは、CellTiter Glo (Promega)で細胞数指標を取り、negative control siRNAを導入した細胞群の四日目の細胞数からsiRNAを導入した翌日の細胞数を引いた値を100%とする。

図3. RT-PCR による融合変異遺伝子 X の発現確認

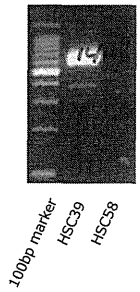

別紙５　研究成果の刊行に関する一覧表

1: Miyanaga A, Honda K, Tsuta K, Masuda M, Yamaguchi U, Fujii G, Miyamoto A, Shinagawa S, Miura N, Tsuda H, Sakuma T, Asamura H, Gemma A, Yamada T.

Diagnostic and prognostic significance of the alternatively spliced ACTN4 variant in high-grade neuroendocrine pulmonary tumours.

Ann Oncol. 2013 Jan;24(1):84-90.

2: Arai E, Chiku S, Mori T, Gotoh M, Nakagawa T, Fujimoto H, Kanai Y.

Single-CpG-resolution methylome analysis identifies clinicopathologically aggressive CpG island methylator phenotype clear cell renal cell carcinomas.

Carcinogenesis. 2012 Aug;33(8):1487-93.

3: Sato T, Arai E, Kohno T, Tsuta K, Watanabe S, Soejima K, Betsuyaku T, Kanai Y.

DNA methylation profiles at precancerous stages associated with recurrence of lung adenocarcinoma.

PLoS One. 2013;8(3):e59444.

4: Huang C, Ding G, Gu C, Zhou J, Kuang M, Ji Y, He Y, Kondo T, Fan J.

Decreased selenium-binding protein 1 enhances glutathione peroxidase 1 activity and downregulates HIF-1α to promote hepatocellular carcinoma invasiveness.

Clin Cancer Res. 2012 Jun 1;18(11):3042-53.

5: Huang C, Wang Y, Liu S, Ding G, Liu W, Zhou J, Kuang M, Ji Y, Kondo T, Fan J.

Quantitative Proteomic Analysis Identified Paraoxonase 1 as a Novel Serum Biomarker for Microvascular Invasion in Hepatocellular Carcinoma.

J Proteome Res. 2013 Mar 5. [Epub ahead of print]

6: Kimura K, Ojima H, Kubota D, Sakumoto M, Nakamura Y, Tomonaga T, Kosuge T, Kondo T.

Proteomic identification of the macrophage-capping protein as a protein contributing to the malignant features of hepatocellular carcinoma.

J Proteomics. 2013 Jan 14;78:362-73.

7: Takeishi S, Matsumoto A, Onoyama I, Naka K, Hirao A, Nakayama KI. Ablation of Fbxw7 eliminates leukemia-initiating cells by preventing quiescence. ***Cancer Cell.*** 2013 Mar 18;23(3):347-61.

8: Hirano A, Yumimoto K, Tsunematsu R, Matsumoto M, Oyama M, Kozuka-Hata H, Nakagawa T, Lanjakornsiripan D, Nakayama KI, Fukada Y. FBXL21 regulates oscillation of the circadian clock through ubiquitination and stabilization of cryptochromes.
Cell. 2013 Feb 28;152(5):1106-18.

Annals of Oncology 24: 84–90, 2013
doi:10.1093/annonc/mds215
Published online 10 August 2012

Diagnostic and prognostic significance of the alternatively spliced *ACTN4* variant in high-grade neuroendocrine pulmonary tumours

A. Miyanaga[1,2], K. Honda[1], K. Tsuta[3], M. Masuda[1], U. Yamaguchi[1], G. Fujii[4], A. Miyamoto[5], S. Shinagawa[5], N. Miura[1], H. Tsuda[3], T. Sakuma[6], H. Asamura[7], A. Gemma[2] & T. Yamada[1]*

[1]*Division of Chemotherapy and Clinical Research, National Cancer Center Research Institute, Tokyo;* [2]*Department of Internal Medicine, Division of Pulmonary Medicine, Infection and Oncology, Nippon Medical School, Tokyo;* [3]*Division of Pathology and Clinical Laboratories, National Cancer Center Hospital, Tokyo;* [4]*Division of Cancer Prevention Research, National Cancer Center Research Institute, Tokyo ;* [5]*Kobe Research Center, TransGenic Inc., Kumamoto;* [6]*BioBusiness Group, Mitsui Knowledge Industry, Tokyo;* [7]*Division of Thoracic Surgery, National Cancer Center Hospital, Tokyo, Japan*

Received 2 April 2012; revised 30 May 2012; accepted 31 May 2012

Background: High-grade neuroendocrine tumours (HGNTs) of the lung manifest a wide spectrum of clinical behaviour, but no method for predicting their outcome has been established.
Materials and methods: We newly established a monoclonal antibody specifically recognizing the product of the alternatively spliced *ACTN4* transcript (namely, variant actinin-4), and used it to examine the expression of variant actinin-4 immunohistochemically in a total of 609 surgical specimens of various histological subtypes of lung cancer.
Results: Variant actinin-4 was expressed in 55% (96/176) of HGNTs, but in only 0.8% (3/378) of non-neuroendocrine (NE) lung cancers. The expression of variant actinin-4 was significantly associated with poorer overall survival in HGNT patients ($P = 0.00021$, log-rank test). Multivariate analysis using the Cox proportional hazards model showed that the expression of variant actinin-4 was the most significant independent negative predictor of survival in HGNT patients (hazard ratio (HR), 2.15; $P = 0.00113$) after the presence of lymph node metastasis (HR, 2.25; $P = 0.00023$).
Conclusions: The expression of variant actinin-4 is an independent prognostic factor for patients with HGNTs. This protein has a high affinity for filamentous actin polymers and likely promotes aggressive behaviour of cancer cells. The present clinical findings clearly support this notion.
Key words: actinin-4, alternative splice variant, diagnostic marker, high-grade neuroendocrine tumour, pulmonary neoplasm, prognosis

introduction

Neuroendocrine (NE) tumours comprise 20%–25% of all human lung malignancies and are classified into four histological subtypes: typical carcinoid (TC), atypical carcinoid (AC), large cell neuroendocrine carcinoma (LCNEC) and small cell lung carcinoma (SCLC) [1, 2]. TC and AC are tumours with low- to intermediate-grade malignancy, whereas LCNEC and SCLC are highly aggressive and collectively referred to as high-grade neuroendocrine tumours (HGNTs) [3–6].

LCNEC appeared in the World Health Organization (WHO) Histological Typing of Lung and Pleural Tumours (third version, 1999) as a new entity of large cell carcinoma [2]. LCNEC shows aggressive behaviour distinct from other non-small cell lung cancers (NSCLCs) [7], and thus its accurate discrimination is essential for the management of lung cancer patients. TC, AC and SCLC can be readily diagnosed on the basis of their histological characteristics, but the diagnosis of LCNEC is more complicated. The morphological features of NE differentiation are often inconspicuous, especially in small biopsy or cytology specimens [2].

Three NE markers are used routinely for immunohistochemical assessment of NE differentiation: neural cell adhesion molecule (CD56), chromogranin A (CGA) and synaptophysin (SYN). However, a significant proportion of LCNECs are negative for any of these NE markers [7], and more problematically, some non-NE lung cancers also show equivocal immunoreactivity for these markers [7, 8]. Therefore, it is necessary to develop a new diagnostic biomarker with higher specificity.

Actinin-4 is an actin-binding protein that we originally identified as being associated with enhanced cell motility and cancer invasion [9]. The actinin-4 (*ACTN4*) gene has a unique structure (supplementary Figure S1, available at *Annals of*

*Correspondence to: Prof. T. Yamada, Division of Chemotherapy and Clinical Research, National Cancer Center Research Institute, 5-1-1 Tsukiji, Chuo-ku, Tokyo 104-0045, Japan. Tel: +81-3-3542-2511; Fax: +81-3-3547-6045; E-mail: tyamada@ncc.go.jp

Oncology online), possessing two exons 8 (8 and 8[?]) of the same size, the mutually exclusive use of which leads to the production of two kinds of mRNA. The transcript obtained with exon 8 is expressed ubiquitously (namely, the ubiquitous form or *ACTN4*-Ub), whereas the expression of the variant transcript obtained with exon 8[?] (the variant form or *ACTN4*-Va) is undetectable in normal tissues except for testis and brain [10, 11]. We previously found that the variant transcript is frequently expressed in SCLCs and that the gene product can be categorized as a so-called cancer-testis antigen [10]. However, the clinical significance of variant actinin-4 has remained undetermined due to lack of a specific probe.

The alternatively spliced actinin-4 variant transcript is predicted to encode a polypeptide differing in only three amino acids. To produce an antibody that can detect this small difference, we used the *GANP* (germinal centre-associated nuclear protein) technology [12]. *GANP* transgenic mice generate a highly diverse spectrum of antibodies and have been used to produce high-affinity antibodies against various difficult antigens, such as those with small protein modifications [13]. Here, we report the establishment of a highly specific antibody recognizing variant actinin-4 protein and the potential utility of variant actinin-4 not only as a new diagnostic biomarker but also as a highly potent prognostic biomarker for HGNTs.

materials and methods

cell lines and sequencing

Total RNA was extracted from 91 human cancer cell lines (31 lung cancers, 23 colorectal cancers, 7 stomach cancers, 5 hepatocellular carcinomas, 6 pancreatic cancers, 4 choriocarcinomas, 4 ovary cancers, 4 oral cancers, 3 prostate cancers, 2 breast cancers, 1 bladder cancer and 1 cervical cancer) using TRIzol reagent (Life Technologies, Grand Island, NY) (supplementary Table S1, available at *Annals of Oncology* online).

First-strand complementary DNA (cDNA) was synthesized in the presence of random primers using the high-capacity cDNA reverse transcription kit (Life Technologies) in accordance with the manufacturer's instructions. The entire coding region of *ACTN4* was amplified and sequenced using the BigDye Terminator v3.1 Cycle Sequencing Ready Reaction Kit (Life Technologies).

production of monoclonal antibodies

GANP transgenic mice were immunized with a synthetic peptide (NQSYQYGPSSAGNGAG) to produce a monoclonal antibody (namely 13G9) reactive with all the known forms (ubiquitous and variant) of actinin-4. Another monoclonal antibody specific to variant actinin-4 (namely 15H2) was raised against a synthetic peptide (DIVGTLRPDEKAIMTYVSC). The reactivity and titre of antibodies against the various peptides were assessed by the antibody capture assay as described previously [13].

western blot analysis

The PCR-amplified fragments encoding the ubiquitous and variant forms of actinin-4 (amino acids 28–911) were cloned into the EcoRI and KpnI sites of the pEGFP-C1 vector (Takara Bio, Otsu, Japan) to express the ubiquitous and variant actinin-4 proteins fused with green fluorescent protein (GFP) at the N-termini (namely pEGFP-ACTN4-Ub and pEGFP-ACTN4-Va, respectively). The nucleotide sequences of all the PCR-amplified fragments were verified by sequencing. HEK293 cells (Health Science Research Resources Bank, Osaka, Japan) were transfected with each plasmid using Lipofectamine 2000 reagent (Life Technologies).

Western blotting was carried out following standard procedures, as described previously [14, 15]. Cells were extracted with lysis buffer [10 mmol/l HEPES (pH 7.4), 150 mmol/l NaCl, 1 mmol/l EDTA, 1% Triton X-100, 1% NP40 and 1 mg/ml NaN_3] containing a protease inhibitor cocktail (Sigma-Aldrich, St. Louis, MO) on ice for 30 min. Ten micrograms of cell lysate were reduced, denatured at 70°C for 10 min and fractionated through NuPAGE 4%–12% Bis-Tris gel (Life Technologies). The fractionated proteins were then blotted onto PVDF membranes (Life Technologies). After incubation with the primary antibody at 4°C overnight, the blots were incubated with appropriate horseradish peroxidase-linked secondary antibodies and then detected by enhanced chemiluminescence (Western Lightning ECL Pro; Perkin-Elmer, Waltham, MA).

patients and tissue samples

Thirty-one tissue microarrays (TMAs) were constructed from formalin-fixed paraffin-embedded tissue blocks of 609 primary lung tumours that had been surgically resected at the National Cancer Center (NCC) Hospital (Tokyo, Japan) from 1982 to 2010 using a tissue-arraying instrument (KIN-1; Azumaya, Tokyo, Japan). Based on the Pathology and genetics of Tumours of the Lung, Pleura, Thymus and Heart [IARC (International Agency for Research on Cancer) WHO Classification of Tumours] (2004) [16], the 609 tumours were classified into carcinoid (51 cases), SCLC (70 cases), LCNEC (106 cases), adenocarcinoma (164 cases), squamous cell carcinoma (166 cases) and other NSCLCs (52 cases). To reduce sampling bias due to tissue heterogeneity, we took duplicate core samples measuring 2.0 mm in diameter from two different areas of every tumour.

The 176 patients with HGNTs included 143 men and 33 women with a mean age of 66 years (19–84 years). One hundred and sixty-nine (96%) patients had a history of habitual cigarette smoking. The follow-up periods ranged from 1 to 286 months (median follow-up, 46 months). Patients were staged postsurgically into IA (52 cases), IB (25 cases), IIA (33 cases), IIB (16 cases), IIIA (37 cases), IIIB (7 cases) and IV (6 cases) according to the International Union against Cancer (UICC) TNM classification of malignant tumours (7th edition, 2010) [17].

This study was conducted with approval from the Institutional Review Board of the NCC.

immunohistochemistry

TMA blocks were then cut into 4-mm thick sections and subjected to immunohistochemistry (IHC). Immunostaining of actinin-4 proteins was carried out using the Ventana DABMap detection kit and an automated slide stainer (Discovery XT, Ventana Medical Systems, Tucson, AZ) [18, 19]. Immunoreactivity was classified as positive when ≥10% of cancer cells showed cytoplasmic or membrane staining detectable at a magnification of ×40 [20, 21].

Deparaffinized TMA slides were incubated with anti-CD56 mouse monoclonal (1B6, Novocastra, Newcastle upon Tyne, UK), anti-CGA rabbit polyclonal (Dako, Glostrup, Denmark) or anti-SYN mouse monoclonal (27G12, Nichirei Biosciences, Tokyo, Japan) antibody for 1 h at room temperature. Immunoreactivity was detected with the EnVision plus kit (Dako) using 3, 3[?]-diaminobenzidine as the chromogen. For diagnosis of LCNEC, positive staining for at least one of the three NE markers was stipulated.

The results of IHC were judged by two investigators (AM and KT) who were blinded to any clinicopathological information, and any discrepancy in judgement was discussed.

statistical analysis

Overall survival was measured as the period from surgery to the date of death or last follow-up. Progression-free survival was defined as the length of time from surgery to the first detection of new lesions or death. Overall and progression-free survival was estimated by the Kaplan–Meier method using the StatFlex statistical software package (version 5.0, Artiteck, Osaka, Japan). Differences between the survival curves were assessed with the log-rank test. Univariate and multivariate analyses were carried out using the Cox regression model. Other statistical tests were carried out using tools available in the R statistical package (version 2.12.0; http://www.r-project.org/). Differences were considered to be statistically significant at $P < 0.05$.

results

expression of the *ACTN4* splice variant in cancer cell lines

We sequenced the entire coding region of the *ACTN4* transcript in 91 cell lines derived from human cancers of various origins (supplementary Table S1, available at *Annals of Oncology* online). No non-synonymous nucleotide substitution was detected except for those registered in the single nucleotide polymorphism database (http://www.ncbi.nlm.nih.gov/snp), indicating that somatic mutation of the *ACTN4* gene is infrequent. However, we detected overlap of two sequences appearing in nucleotides 793–872 of the *ACTN4* transcript (NM_004924.2) (supplementary Figure S2A, available at *Annals of Oncology* online) in 25% (23/91) of the cell lines. These two transcripts were separately cloned, and their nucleotide sequences were confirmed to be identical to the ubiquitous and variant transcripts of *ACTN4* that we had described previously [10] (supplementary Figure S2B, available at *Annals of Oncology* online).

The ubiquitous form of the *ACTN4* transcript (namely *ACTN4*-Ub) was expressed in all of the 91 human cancer cell lines examined, but the variant form (namely *ACTN4*-Va) was detected in 90% (18/20) of the SCLC cell lines examined (SBC-3, SBC-5, MS-1-L, Lu-135, Lu-143, STC-1, Lu-138, Lu-140, DMS153, DMS53, H1688, Wa-hT, H69AR, RERF-LCMS, Lu165, H69, Lu134-AH, Lu134-B, Lu-141 and Lu-139) and 25% (1/4) of the cell lines derived from pulmonary carcinoid tumour (NCI-H727, NCI-H835, UMC-11 and NCI-H720) (supplementary Table S1, available at *Annals of Oncology* online). In addition, the variant *ACTN4* mRNA was detected in 33% (1/3) of prostate cancers and 75% (3/4) of choriocarcinoma cell lines. However, none of the seven non-SCLC-derived cell lines examined (A549, PC9, LCD, LCKJ, LK-2, Lu-65 and Lu-99) expressed the variant transcript.

production of antibody specific to variant actinin-4 protein

Although there was a difference of only three amino acid residues between the ubiquitous and variant actinin-4 protein sequences deduced from their cDNA sequences (supplementary Figure S2C, available at *Annals of Oncology* online), we were able to produce a monoclonal antibody (15H2) that reacted specifically with a peptide for which the amino acid sequence was derived from the variant actinin-4 protein (DIVGTLRPDEKAIMTYVSC), but not with the corresponding sequence of the ubiquitous protein (DIVNTARPDEKAIMTYVSS) (underlining indicates the amino acids that differed) (Figure 1A).

To further confirm that the 15H2 monoclonal antibody reacted specifically with the variant form of actinin-4 protein, HEK 293 cells were transfected with a plasmid encoding the ubiquitous (pEGFP-ACTN4-Ub) or variant (pEGFP-ACTN4-Va) form of actinin-4. We found that the 15H2 antibody reacted only with a lysate prepared from HEK 293 cells transfected with pEGFP-ACTN4-Va, but not with those prepared from cells transfected with pEGFP-ACTN4-Ub or the parental pEGFP-C1 vector (ACTN4-Va, Figure 1B). On the other hand, the monoclonal antibody 13G9 reacted with both the ubiquitous and variant actinin-4 proteins (pan-ACTN4, Figure 1B).

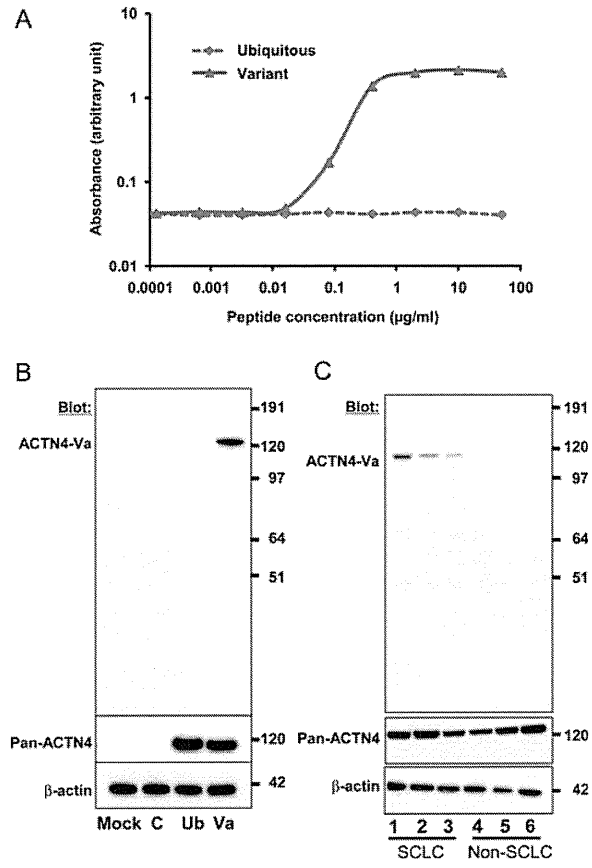

Figure 1. Specificity of the 15H2 monoclonal antibody to the actinin-4 variant. (A) Reactivity of the 15H2 monoclonal antibody with the synthetic peptides DIVNTARPDEKAIMTYVSS (ubiquitous) and DIVGTLRPDEKAIMTYVSC (variant), as determined by the antibody capture assay. (B) Proteins were extracted from HEK293 cells that had been transfected with no plasmid (mock), pEGFP (C), pEGFP-ACTN4-Ub (Ub) or pEGFP-ACTN4-Va (Va) and blotted with 15H2 (ACTN4-Va), 13G9 (pan-ACTN4) and anti-β-actin (loading control) antibodies. Molecular masses (in kiloDaltons) are shown on the right. (C) Proteins were extracted from three small cell lung carcinoma (SCLC) cell lines [SBC3- (lane 1), Lu-135 (2) and Lu-165 (3)] and three non-small cell lung carcinoma (NSCLC) cell lines [LCD (4), LK-2 (5) and EBC-1 (6)] and blotted with 15H2 (ACTN4-Va), 13G9 (pan-ACTN4) and anti-β-actin (loading control) antibodies. Molecular masses (in kiloDaltons) are shown on the right.

Table 3. Hazard ratios for death in patients with high-grade neuroendocrine tumours

Variable		Univariate analysis			Multivariate analysis		
	N	HR	95% CI	*P* value	HR	95% CI	*P* value
Age							
< 65/≥65 years	71/102	1.00	0.65–1.55	0.983			
Smoking history							
Absent/present	7/166	1.63	0.40–6.65	0.492			
Gender							
Female/male	33/140	1.12	0.64–1.96	0.683			
Tumour size							
≤3 cm/>3 cm	93/80	1.33	0.87–2.04	0.184			
Lymph node metastasis							
Absent/present	101/72	2.37	1.54–3.65	0.00008	2.25	1.46–3.47	0.00023
Distant metastasis							
Absent/present	167/6	1.70	0.69–4.20	0.249			
Adjuvant chemotherapy							
Yes/no	40/133	0.77	0.44–1.35	0.362			
Histological subtype							
LCNEC/SCLC	103/70	1.12	0.73–1.74	0.596			
Variant actinin-4 protein expression							
Negative/positive	79/94	2.27	1.43–3.59	0.000467	2.15	1.36–3.40	0.00113

Three patients with LCNEC, for whom no data regarding adjuvant therapy were available, were excluded from the analysis.
HR, hazard ratio; CI, confidence interval; LCNEC, large cell neuroendocrine carcinoma; SCLC, small cell lung carcinoma.

is not a simple marker for NE differentiation, but seems to be associated with the malignant progression of NE tumours.

We originally identified actinin-4 as an actin-bundling protein associated with enhanced cell motility and cancer invasion [9]. Actinin-4 directly regulates cell motility through remodelling of the actin cytoskeleton [9, 22]. Increased expression of actinin-4 protein is closely associated with a poor outcome in patients with breast cancer [9], colorectal cancer [22], pancreatic cancer [18], ovarian cancer [19] and NSCLC [23]. However, the expression of total actinin-4 protein (i.e. the ubiquitous and variant actinin-4 proteins together) detected by the monoclonal antibody 13G9 was not significantly correlated with the outcome of HGNT patients (supplementary Figure S4, available at *Annals of Oncology* online). The amino acid sequence encoded by exon 8 is crucial for the function of the *ACTN4* gene. In fact, a germline missense mutation in exon 8 is responsible for a hereditary renal disease, familial focal segmental glomerulosclerosis [24]. The splice variant as well as mutated actinin-4 proteins have a higher affinity for actin polymers [10]. SCLC shows an abnormal actin cytoskeleton structure [10]. Existing experimental data as well as the current clinical observations suggest that variant actinin-4 very likely plays a functional role in the aggressive behaviour of NE lung tumours. Because of its limited expression in normal tissues, variant actinin-4 may also serve as a therapeutic target.

If a biomarker capable of defining a subset of HGNT patients whose prognosis is likely to be unfavourable were to be identified, allowing them to be selected for intense adjuvant chemotherapy, then their survival might be improved. Recently Klotho was newly characterized as a biomarker predictive of a favourable outcome in patients with LCNEC [25] and limited-disease SCLC [26], although the number of cases examined was relatively small. The expression of CD117 was also reported to show marginally significant correlation with recurrence of LCNEC ($P = 0.046$) [27]. It is expected that combination of these emerging prognostic biomarkers with variant actinin-4 would further improve the accuracy of HNGT prognostication. Future investigation to select and validate an optimal biomarker set is anticipated.

funding

This study was supported by the Program for Promotion of Fundamental Studies in Health Sciences conducted by the National Institute of Biomedical Innovation of Japan, Research on Biological Markers for New Drug Development conducted by the Ministry of Health, Labor and Welfare of Japan and the National Cancer Center Research and Development Fund.

disclosure

The authors have declared no conflicts of interest.

references

1. Travis WD, Linnoila RI, Tsokos MG et al. Neuroendocrine tumors of the lung with proposed criteria for large-cell neuroendocrine carcinoma. An ultrastructural, immunohistochemical, and flow cytometric study of 35 cases. Am J Surg Pathol 1991; 15: 529–553.
2. Travis WD, Colby TV, Corrin B et al. World Health Organization International Histological Classification of Tumors. Histological Typing of Lung and Pleural Tumors, 3rd edition. Berlin: Springer 1999.
3. Cooper WA, Thourani VH, Gal AA et al. The surgical spectrum of pulmonary neuroendocrine neoplasms. Chest 2001; 119: 14–18.
4. Travis WD, Rush W, Flieder DB et al. Survival analysis of 200 pulmonary neuroendocrine tumors with clarification of criteria for atypical carcinoid and its separation from typical carcinoid. Am J Surg Pathol 1998; 22: 934–944.

Table 2. Association of expression of the actinin-4 variant with clinicopathological characteristics of high-grade neuroendocrine tumour (HGNT) patients

Characteristic	Total	Actinin-4 splice variant		*P* value[a]
		Positive (%)	Negative (%)	
Sex				
Male	143	78 (55%)	65 (46%)	1
Female	33	18 (55%)	15 (46%)	
Age				
≥65 years	105	60 (57%)	45 (43%)	0.442
<65 years	71	36 (51%)	35 (49%)	
Smoking status				
Never smoked	7	3 (43%)	4 (57%)	0.703
Current or former smoker	169	93 (55%)	76 (45%)	
Histological subtype				
SCLC	70	42 (60%)	28 (40%)	0.280
LCNEC	106	54 (51%)	52 (49%)	
Pathological stage[b]				
I, II	124	62 (50%)	62 (50%)	0.069
III, IV	52	34 (65%)	18 (35%)	
Tumour size				
≤3 cm	94	56 (60%)	38 (40%)	0.173
>3 cm	82	40 (49%)	42 (51%)	
Lymph node metastasis				
Absent	101	50 (50%)	51 (51%)	0.129
Present	75	46 (61%)	29 (39%)	
Distant metastasis				
Absent	170	92 (54%)	78 (46%)	0.690
Present	6	4 (67%)	2 (33%)	
Recurrence				
Absent	91	39 (43%)	52 (57%)	**0.00200**
Present	79	53 (67%)	26 (33%)	

SCLC, small cell lung carcinoma; LCNEC, large cell neuroendocrine carcinoma.

[a]Fisher's exact test. *P* values of < 0.05 are shown in bold.

[b]According to the International Union Against Cancer (UICC) TNM Classification of Malignant Tumours, 7th edition (2010).

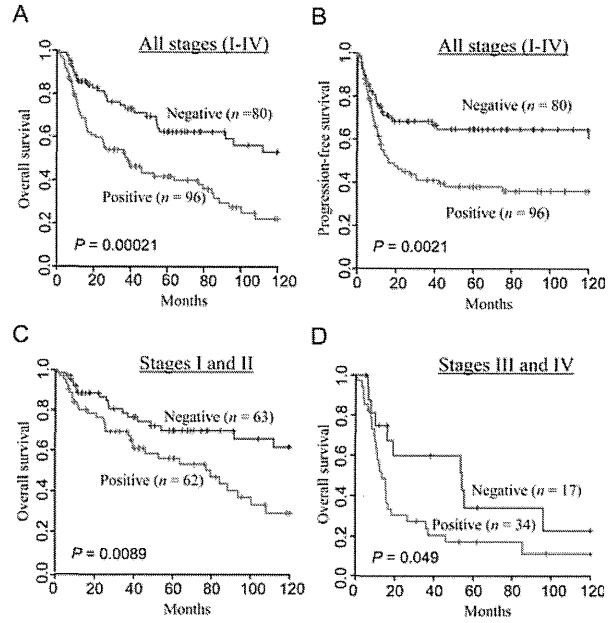

Figure 3. Survival of high-grade neuroendocrine tumour (HGNT) patients according to expression of the actinin-4 variant protein. Kaplan–Meier estimates of overall (A, C and D) and progression-free (B) survival for patients with all stages (A and B), stages I and II (C) and stages III and IV (D) HGNTs. Differences between the curves were assessed using the log-rank test.

patients whose tumours were positive were 42%, 32% and 49%, respectively. The prognostic significance of variant actinin-4 protein expression was reproducibly observed in subgroup analyses of patients with stages I and II and stages III and IV HGNT ($P = 0.0089$ and $P = 0.049$, respectively) (Figure 3C and D), whereas the expression of total actinin-4 proteins (detected by 13G9 monoclonal antibody) (supplementary Figure S4, available at *Annals of Oncology* online) or the three conventional NE markers (CGA, SYN and CD56) (supplementary Figure S5, available at *Annals of Oncology* online) did not show such prognostic significance.

Univariate analysis with the Cox proportional hazards model (Table 3) revealed that lymph node metastasis ($P = 0.000082$) and immunoreactivity for the actinin-4 splice variant ($P = 0.000467$) were significantly correlated with the outcome of the 173 patients with HGNTs. Multivariate analysis indicated that the expression of the actinin-4 splice variant was the most significant independent predictor of unfavourable outcome ($P = 0.00113$; hazard ratio (HR), 2.15; 95% confidence interval (CI) 1.36–3.40) after the presence of lymph node metastasis ($P = 0.00023$; HR, 2.25; 95% CI 1.46–3.47). The variant actinin-4 protein expression was also a significant independent predictor of outcome for SCLC (supplementary Table S2, available at *Annals of Oncology* online) ($P = 0.050$; HR, 2.16; 95% CI 1.00–4.68) and LCNEC (supplementary Table S3, available at *Annals of Oncology* online) ($P = 0.0038$; HR, 2.37; 95% CI 1.32–4.26).

discussion

In this study, we first determined the distribution of expression of the alternatively spliced *ACTN4* transcript in a large panel of human cancer cell lines derived from various tissues. We confirmed the frequent expression of *ACTN*-Va in SCLCs and the absence of its expression in NSCLCs. The variant transcript was also expressed frequently in choriocarcinoma, but its relationship with NE differentiation as well as its clinical significance remained undetermined. We then investigated the expression of the variant actinin-4 protein in a variety of histological subtypes of lung cancer using a newly established monoclonal antibody (Figure 1). We found that the expression pattern of the variant protein was apparently different from any of the conventional NE markers. CGA, SYN and CD56 were expressed in 76%–100% of pulmonary carcinoid tumours (Table 1), whereas the variant actinin-4 was expressed in only 10% (5/51) of them. The expression of variant actinin-4, but not that of CGA, SYN or CD56, was significantly associated with an unfavourable post-surgical outcome in HGNT patients (Figure 3 and supplementary Figure S5, available at *Annals of Oncology* online). These results indicated that variant actinin-4

The expression of endogenous variant actinin-4 was detected in all three SCLC cell lines examined (SBC-3, Lu-135 and Lu-165), but in none of the three non-SCLC cell lines (LCD, LK-2 and EBC-1) (Figure 1C), being consistent with the results of cDNA sequencing described above.

significance of variant actinin-4 expression in the diagnosis of HGNT

We next investigated immunohistochemically the expression of both actinin-4 proteins and classical NE markers (CGA, SYN and CD56) in 609 primary lung tumours. Representative results of immunohistochemical staining are shown in Figure 2, and the positivity rates for each histological subtype are summarized in Table 1. CGA was expressed in 88% (59/67) of SCLCs and 56% (59/105) of LCNECs. SYN was expressed in 88% (58/66) of SCLCs and 56% (59/105) of LCNECs. CD56 was expressed in 96% (64/67) of SCLCs and 72% (76/105) of LCNECs. The three NE markers were also expressed in 76%–100% of pulmonary carcinoid tumours (Table 1). The expression of variant actinin-4 protein was detected in 55% (96/176) of HGNTs [60% (42/70) of SCLCs and 51% (54/106) of LCNECs], but in only 10% (5/51) of carcinoid tumours. The difference in the frequency of variant actinin-4 expression between HGNTs and carcinoid tumours was statistically significant ($P = 6.0 \times 10^{-6}$, Fisher's exact test).

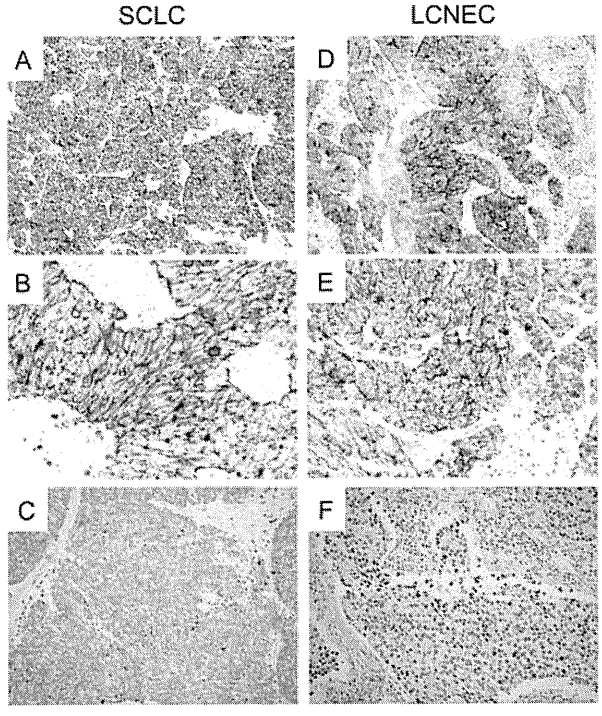

Figure 2. Expression of the variant actinin-4 protein in high-grade neuroendocrine tumour (HGNT). Representative cases of small cell lung carcinoma (SCLC) (A–C) and large cell neuroendocrine carcinoma (LCNEC) (D–F) showing positive (A, B, D and E) and negative (C and F) immunoreactivity with the 15H2 monoclonal antibody. Original magnification: A, C, D and F, ×20; B and E, ×400.

CGA, SYN and CD56 were found to show variable expression in non-NE lung tumours (2%–11% of adenocarcinomas, 2%–14% of squamous cell carcinomas and 6%–17% of other NSCLCs). However, variant actinin-4 protein was expressed in only 0.8% (3/382) of non-NE NSCLCs. These results indicated that variant actinin-4 was highly specific to HGNTs.

prognostic significance of variant actinin-4 expression

There was no significant difference between patients with HGNTs that were positive ($n = 96$) and negative ($n = 80$) for variant actinin-4 protein expression with respect to gender, age, smoking status, histological subtype (LCNEC versus SCLC), pathological stage, tumour size or frequency of lymph node or distant metastasis (Table 2). However, the frequency of relapse after surgery was much higher in stage I to III HGNT cases that were positive for variant actinin-4 protein expression [67% (53/79)] than in cases that were negative [43% (39/91)] ($P = 0.0020$, Fisher's exact test) (Table 2). The sites of first recurrence in patients with HGNTs that were positive for variant actinin-4 expression included the brain (16 cases), lymph nodes (16 cases), lung (9 cases), liver (6 cases), and bone (5 cases), but the site distribution did not differ significantly from that in negative cases.

The overall survival of patients with variant actinin-4-positive HGNT, SCLC and LCNEC was significantly worse than that of patients whose tumours were negative [$P = 0.00021$ (HGNT, Figure 3A), 0.0283 (SCLC, supplementary Figure S3A, available at *Annals of Oncology* online) and 0.0022 (LCNEC, supplementary Figure S3B, available at *Annals of Oncology* online), log-rank test]. Furthermore, progression-free survival also differed significantly between patients whose tumours were positive and negative for variant actinin-4 expression [$P = 0.0021$ (HGNT, Figure 3B), 0.018 (SCLC, supplementary Figure S3C, available at *Annals of Oncology* online) and 0.048 (LCNEC, supplementary Figure S3D, available at *Annals of Oncology* online), log-rank test]. The 5-year survival rates of patients with variant actinin-4-negative HGNT, SCLC and LCNEC were 62%, 62% and 62%, respectively, whereas those of

Table 1. Expression of variant actinin-4 and three NE markers in various histological subtypes of lung cancer

Histological subtype[a]	*N*	Variant actinin-4	CGA	SYN	CD56
SCLC	70	42 (60%)	59 (88%)	58 (88%)	64 (96%)
LCNEC	106	54 (51%)	59 (56%)	59 (56%)	76 (72%)
Carcinoid	51	5 (10%)	49 (100%)	49 (100%)	37 (76%)
Adenocarcinoma	164	1 (1%)	16 (11%)	6 (4%)	4 (2%)
Squamous cell carcinoma	166	2 (1%)	23 (14%)	4 (2%)	16 (10%)
Others	52	0 (0%)	9 (17%)	5 (10%)	3 (6%)

SCLC, small cell lung carcinoma; LCNEC, large cell neuroendocrine carcinoma; NE, neuroendocrine; CGA, chromogranin A; SYN, synaptophysin; IARC, International Agency for Research on Cancer; WHO, World Health Organization.

[a]Based on the Pathology and Genetics of Tumours of the Lung, Thymus and Heart (IARC WHO Classification of tumours) (third version, 2004).

5. Asamura H, Kameya T, Matsuno Y et al. Neuroendocrine neoplasms of the lung: a prognostic spectrum. J Clin Oncol 2006; 24: 70–76.
6. Travis WD. Advances in neuroendocrine lung tumors. Ann Oncol 2010; 21(Suppl 7): vii65–vii71.
7. Takei H, Asamura H, Maeshima A et al. Large cell neuroendocrine carcinoma of the lung: a clinicopathologic study of eighty-seven cases. J Thorac Cardiovasc Surg 2002; 124: 285–292.
8. Ionescu DN, Treaba D, Gilks CB et al. Nonsmall cell lung carcinoma with neuroendocrine differentiation—an entity of no clinical or prognostic significance. Am J Surg Pathol 2007; 31: 26–32.
9. Honda K, Yamada T, Endo R et al. Actinin-4, a novel actin-bundling protein associated with cell motility and cancer invasion. J Cell Biol 1998; 140: 1383–1393.
10. Honda K, Yamada T, Seike M et al. Alternative splice variant of actinin-4 in small cell lung cancer. Oncogene 2004; 23: 5257–5262.
11. Pio R, Montuenga LM. Alternative splicing in lung cancer. J Thorac Oncol 2009; 4: 674–678.
12. Sakaguchi N, Kimura T, Matsushita S et al. Generation of high-affinity antibody against T-cell-dependent antigen in the Ganp gene-transgenic mouse. J Immunol 2005; 174: 4485–4494.
13. Ono M, Matsubara J, Honda K et al. Prolyl 4-hydroxylation of alpha-fibrinogen: a novel protein modification revealed by plasma proteomics. J Biol Chem 2009; 284: 29041–29049.
14. Matsubara J, Ono M, Negishi A et al. Identification of a predictive biomarker for hematologic toxicities of gemcitabine. J Clin Oncol 2009; 27: 2261–2268.
15. Satow R, Shitashige M, Jigami T et al. β-Catenin inhibits promyelocytic leukemia protein tumor suppressor function in colorectal cancer cells. Gastroenterology 2012; 142: 572–581.
16. Travis WD, Brambilla E, Muller-Hermelink HK. World Health Organization Classification of Tumours. Pathology and Genetics of Tumours of the Lung, Pleura, Thymus and Heart. Lyon: IARC Press 2004.
17. Sobin L, Gospodarowicz M, Wittrkind C. TNM Classification of Malignant Tumors. New York: Wiley-Blackwell 2010.
18. Kikuchi S, Honda K, Tsuda H et al. Expression and gene amplification of actinin-4 in invasive ductal carcinoma of the pancreas. Clin Cancer Res 2008; 14: 5348–5356.
19. Yamamoto S, Tsuda H, Honda K et al. Actinin-4 expression in ovarian cancer: a novel prognostic indicator independent of clinical stage and histological type. Mod Pathol 2007; 20: 1278–1285.
20. Idogawa M, Yamada T, Honda K et al. Poly(ADP-ribose) polymerase-1 is a component of the oncogenic T-cell factor-4/beta-catenin complex. Gastroenterology 2005; 128: 1919–1936.
21. Yamaguchi U, Nakayama R, Honda K et al. Distinct gene expression-defined classes of gastrointestinal stromal tumor. J Clin Oncol 2008; 26: 4100–4108.
22. Honda K, Yamada T, Hayashida Y et al. Actinin-4 increases cell motility and promotes lymph node metastasis of colorectal cancer. Gastroenterology 2005; 128: 51–62.
23. Yamagata N, Shyr Y, Yanagisawa K et al. A training-testing approach to the molecular classification of resected non-small cell lung cancer. Clin Cancer Res 2003; 9: 4695–4704.
24. Kaplan JM, Kim SH, North KN et al. Mutations in ACTN4, encoding alpha-actinin-4, cause familial focal segmental glomerulosclerosis. Nat Genet 2000; 24: 251–256.
25. Usuda J, Ichinose S, Ishizumi T et al. Klotho is a novel biomarker for good survival in resected large cell neuroendocrine carcinoma of the lung. Lung Cancer 2011; 72: 355–359.
26. Usuda J, Ichinose S, Ishizumi T et al. Klotho predicts good clinical outcome in patients with limited-disease small cell lung cancer who received surgery. Lung Cancer 2011; 74: 332–337.
27. Casali C, Stefani A, Rossi G et al. The prognostic role of c-kit protein expression in resected large cell neuroendocrine carcinoma of the lung. Ann Thorac Surg 2004; 77: 247–252.

Annals of Oncology 24: 90–96, 2013
doi:10.1093/annonc/mds281
Published online 16 August 2012

Phase Ib safety and pharmacokinetic study of volociximab, an anti-α5β1 integrin antibody, in combination with carboplatin and paclitaxel in advanced non-small-cell lung cancer

B. Besse[1]*, L. C. Tsao[2], D. T. Chao[3], Y. Fang[4], J.-C. Soria[5,6], S. Almokadem[7] & C. P. Belani[7]

[1]Cancer Medicine/Thoracic Unit, Institut Gustave Roussy, Villejuif, France; Departments of [2]Biometry; [3]Discovery, GPRD; [4]Bio-analytical Sciences, Department of Preclinical and Clinical Development Sciences, Abbott Biotherapeutics Corp., Redwood City, USA; [5]Cancer Medecine/Service des Innovations Thérapeutiques Précoces, Institut Gustave Roussy, Villejuif, France; [6]Université Paris-Sud 11, Orsay, France; [7]Department of Medicine, Division of Medical Oncology, Penn State Hershey Cancer Institute, Hershey, USA

Received 14 February 2012; revised 15 May 2012; accepted 20 June 2012

Background: This phase Ib study evaluated volociximab, an anti-α5β1 integrin antibody, in combination with carboplatin (Eli Lilly and Co., Indianapolis, IN) and paclitaxel (Taxol) in advanced, untreated non-small-cell lung cancer (NSCLC).

*Correspondence to: Dr B. Besse, Department of Oncology Medicine/Thoracic Unit, Institut Gustave Roussy, Villejuif Cedex 94805, France. Tel: +33-1-42114322; Fax: +33-1-42-11-52-19; E-mail: benjamin.besse@igr.fr

Carcinogenesis vol.33 no.8 pp.1487–1493, 2012
doi:10.1093/carcin/bgs177
Advance Access Publication May 18, 2012

Single-CpG-resolution methylome analysis identifies clinicopathologically aggressive CpG island methylator phenotype clear cell renal cell carcinomas

Eri Arai[1], Suenori Chiku[2], Taisuke Mori[1], Masahiro Gotoh[1], Tohru Nakagawa[3], Hiroyuki Fujimoto[3] and Yae Kanai[1,*]

[1]Division of Molecular Pathology, National Cancer Center Research Institute, Tokyo 104-0045, Japan, [2]Science Solutions Division, Mizuho Information and Research Institute, Inc., Tokyo 101-8443, Japan and [3]Department of Urology, National Cancer Center Hospital, Tokyo 104-0045, Japan

*To whom correspondence should be addressed. Tel: +81 3 3542 2511; Fax: +81 3 3248 2463; Email: ykanai@ncc.go.jp

To clarify the significance of DNA methylation alterations during renal carcinogenesis, methylome analysis using single-CpG-resolution Infinium array was performed on 29 normal renal cortex tissue (C) samples, 107 non-cancerous renal cortex tissue (N) samples obtained from patients with clear cell renal cell carcinomas (RCCs) and 109 tumorous tissue (T) samples. DNA methylation levels at 4830 CpG sites were already altered in N samples compared with C samples. Unsupervised hierarchical clustering analysis based on DNA methylation levels at the 801 CpG sites, where DNA methylation alterations had occurred in N samples and were inherited by and strengthened in T samples, clustered clear cell RCCs into Cluster A (n = 90) and Cluster B (n = 14). Clinicopathologically aggressive tumors were accumulated in Cluster B, and the cancer-free and overall survival rates of patients in this cluster were significantly lower than those of patients in Cluster A. Clear cell RCCs in Cluster B were characterized by accumulation of DNA hypermethylation on CpG islands and considered to be CpG island methylator phenotype (CIMP)-positive cancers. DNA hypermethylation of the CpG sites on the FAM150A, GRM6, ZNF540, ZFP42, ZNF154, RIMS4, PCDHAC1, KHDRBS2, ASCL2, KCNQ1, PRAC, WNT3A, TRH, FAM78A, ZNF671, SLC13A5 and NKX6-2 genes became hallmarks of CIMP in RCCs. On the other hand, Cluster A was characterized by genome-wide DNA hypomethylation. These data indicated that DNA methylation alterations at precancerous stages may determine tumor aggressiveness and patient outcome. Accumulation of DNA hypermethylation on CpG islands and genome-wide DNA hypomethylation may each underlie distinct pathways of renal carcinogenesis.

Introduction

Clear cell renal cell carcinoma (RCC) is the most common histological subtype of adult kidney cancer and frequently affects working-age adults in midlife. In general, RCCs at an early stage are curable by nephrectomy. However, some RCCs relapse and metastasize to distant organs, even if the resection has been considered complete (1). Such clinicopathological diversity may be attributable to distinct pathways of renal carcinogenesis (2). It is well known that clear cell RCCs are characterized by inactivation of the Von Hippel–Lindau tumor-suppressor gene (3). In addition, systematic resequencing and exome analysis of RCCs are now being performed by The Cancer Genome Atlas (4), The Cancer Genome Project (5) and other international efforts (6). Such efforts have revealed that renal carcinogenesis involves inactivation of histone-modifying genes, such as SETD2 (7), a histone H3 lysine 36 methyltransferase, JARIDIC (KDM5C (7)), a histone H3 lysine 4 demethylase, and UTX (KMD6A (8)), a histone H3 lysine 27 demethylase, as well as the SWI/SNF chromatin-remodeling complex gene, PBRM1 (9). Non-synonymous mutations of the NF2 gene and truncating mutations of the MLL2 gene have also been reported (7). However, such gene mutations cannot fully explain the clinicopathological diversity of clear cell RCCs.

Not only genetic, but also epigenetic events appear to accumulate during carcinogenesis, and both types of event reflect the clinicopathological diversity of cancers in various organs in association with each other (10–12). DNA methylation alterations are one of the most consistent epigenetic changes in human cancers (13–16). In fact, on the basis of methylation-specific PCR (MSP), combined bisulfite restriction enzyme analysis (17,18) and bacterial artificial chromosome array-based methylated CpG island amplification (BAMCA (19,20)), we have suggested that non-cancerous renal cortex tissue obtained from patients with RCCs is already at the precancerous stage associated with DNA methylation alterations, even though no remarkable histological changes are evident and there is no association with chronic inflammation or persistent infection with viruses or other pathogenic microorganisms. Genome-wide analysis using BAMCA revealed that DNA methylation status in non-cancerous renal cortex tissue at the precancerous stage was basically inherited by the corresponding clear cell RCC in individual patients (19). DNA methylation alterations at the precancerous stage may confer further susceptibility to genetic and epigenetic alterations and generate more malignant clear cell RCCs (2,13). However, in our previous studies using BAMCA, the resolution and the number of probes were limited. Therefore, further analysis is needed to clarify the significance of DNA methylation alterations in renal carcinogenesis.

Recently, methylome analysis using the Infinium array has made it possible to interrogate 27 000 highly informative CpG sites at single-CpG resolution (21). In order to clarify the significance of DNA methylation alterations during renal carcinogenesis, we used the Infinium BeadChip system to perform genome-wide DNA methylation analysis of 29 samples of normal renal cortex tissue (C) obtained from patients without any primary renal tumors, 107 samples of non-cancerous renal cortex tissue (N) from patients with clear cell RCCs and 109 samples of tissue from the tumors (T) themselves. Correlations between the genome-wide DNA methylation profiles and clinicopathological parameters were then examined.

Abbreviations: BAMCA, bacterial artificial chromosome array-based methylated CpG island amplification; C, normal renal cortex tissue obtained from patients without any primary renal tumor; CIMP, CpG island methylator phenotype; HCC, hepatocellular carcinoma; N, non-cancerous renal cortex tissue obtained from patients with clear cell renal cell carcinomas; NCBI, National Center for Biotechnology Information; RCC, renal cell carcinoma; T, tumorous tissue; TNM, Tumor-Node-Metastasis.

Materials and methods

Patients and tissue samples

The 109 T samples and corresponding 107 N samples showing no remarkable histological changes were obtained from materials that had been surgically resected from 110 patients with primary clear cell RCCs. These patients did not receive preoperative treatment and underwent nephrectomy at the National Cancer Center Hospital, Tokyo, Japan. There were 79 men and 31 women with a mean (±SD) age of 62.8 ± 10.3 years (range 36–85 years). Histological diagnosis was made in accordance with the World Health Organization classification (22) (Supplementary Figure S1, available at *Carcinogenesis* Online). All the tumors were graded on the basis of criteria described previously (23) and classified according to the pathological Tumor-Node-Metastasis (TNM) classification (24). The criteria for macroscopic configuration of RCC (17–19) followed those established for hepatocellular carcinoma (HCC): type 3 (contiguous multinodular type) HCCs show poorer histological differentiation and a higher incidence of intrahepatic metastasis than type 1 (single nodular type) and type 2 (single nodular type with extranodular growth) HCCs (25). The presence or absence of vascular involvement was examined microscopically on slides stained with hematoxylin–eosin and elastica van Gieson. The presence or absence of tumor thrombi in the main trunk of the renal vein was examined macroscopically.

RCC is usually enclosed by a fibrous capsule and well demarcated, and hardly ever contains fibrous stroma between cancer cells. Therefore, we were able to obtain cancer cells from surgical specimens, avoiding contamination with both non-cancerous epithelial cells and stromal cells.

For comparison, 29 samples of normal renal cortex tissue (C1–C29) were obtained from materials that had been surgically resected from 29 patients without any primary renal tumor. These patients included 18 men and 11 women with a mean (±SD) age of 61.4±10.8 years (range 31–81 years). Of these patients, 22 had undergone nephroureterectomy for urothelial carcinomas of the renal pelvis and ureter, 6 had undergone nephrectomy with resection of retroperitoneal sarcoma around the kidney, and the remaining 1 had undergone paraaortic lymph node dissection for metastatic germ cell tumor, which resulted in simultaneous nephrectomy because it was not possible to preserve the renal artery.

All patients included in this study provided written informed consent, and the study was approved by the Ethics Committee of the National Cancer Center, Tokyo, Japan.

Infinium assay

High-molecular-weight DNA from fresh frozen tissue samples was extracted using phenol–chloroform, followed by dialysis (26). Five-hundred-nanogram aliquots of DNA were subjected to bisulfite conversion using an EZ DNA Methylation-Gold™ Kit (Zymo Research, Irvine, CA). Subsequently DNA methylation status at 27 578 CpG loci was examined at single-CpG resolution using the Infinium HumanMethylation27 Bead Array (Illumina, San Diego, CA). This array contains CpG sites located within the proximal promoter regions of the transcription start sites of 14 475 consensus coding sequences in the National Center for Biotechnology Information Database. On average, two assays were selected per gene, and from 3 to 20 CpG sites for more than 200 cancer-related and imprinted genes. Forty control probes were employed for each array; these included staining, hybridization, extension, bisulfite conversion and negative controls. An Evo robot (Tecan, Switzerland) was used for automated sample processing. Whole-genome amplification was performed using the Infinium Assay Kit (Illumina (21)). After hybridization, the specifically hybridized DNA was fluorescence labeled by a single-base extension reaction and detected using a BeadScan reader (Illumina) in accordance with the manufacturer's protocols. The data were then assembled using GenomeStudio methylation software (Illumina). At each CpG site, the ratio of the fluorescent signal was measured using a methylated probe relative to the sum of the methylated and unmethylated probes, i.e. the so-called β-value, which ranges from 0.00 to 1.00, reflecting the methylation level of an individual CpG site.

Statistics

In the Infinium assay, the call proportions (*P*-values for detection of signals above the background <0.01) for 32 probes (shown in Supplementary Table S1, available at *Carcinogenesis* Online) in all of the tissue samples examined were less than 90%. Since such a low proportion may be attributable to polymorphism at the probe CpG sites, these 32 probes were excluded from the present assay. In addition, all CpG sites on chromosomes X and Y were excluded, to avoid any gender-specific methylation bias, leaving a final total of 26 454 autosomal CpG sites.

Infinium probes showing significant differences in DNA methylation levels between the 29 C and 107 N samples were identified by a logistic model adjusted by sex, age and experimental batch. Ordered differences from 29 C to 107 N and then to 109 T samples themselves were examined by the cumulative logit model adjusted by sex, age and experimental batch. Differences of DNA methylation status between 104 paired samples of N and the corresponding T obtained from a single patient and assayed in the same experimental batch were examined by Wilcoxon matched pairs test. A false discovery rate (FDR) of $q = 0.01$ was considered significant. Unsupervised hierarchical clustering (Euclidan distance, Ward method) based on DNA methylation levels ($\Delta\beta_{T-N}$) was performed in patients with clear cell RCCs. Correlations between clusters of patients and clinicopathological parameters were examined using Wilcoxon rank sum test and Fisher's exact test. Survival curves of patients belonging to each cluster were calculated by the Kaplan–Meier method, and the differences were compared by the log-rank test. The number of Infinium assay probes showing DNA hyper- or hypomethylation in each cluster and the average DNA methylation levels ($\Delta\beta_{T-N}$) of each cluster were examined using Wilcoxon rank sum test at a significance level of $P < 0.05$. The CpG sites discriminating the clusters were identified by Fisher's exact test and random forest analysis (27).

Results

DNA methylation alterations during renal carcinogenesis

First, DNA methylation levels of representative CpG sites based on the Infinium assay were clearly verified using a highly quantitative pyrosequencing method (Supplementary Figure S2, available at *Carcinogenesis* Online). With regard to the well-known methylation-silencing Von Hippel–Lindau tumor-suppressor gene (probe Target ID: cg22782492), DNA hypermethylation ($\Delta\beta_{T-N} > 0.1$) was detected in 12 (12%) of 104 patients, for whom both N and T samples were assayed in the same experimental batch. This incidence corresponded to that in previous reports (28,29). Taken together, the data confirmed the reliability of the present Infinium assay.

Although precancerous conditions in the kidney have been rarely described, our previous study suggested that N samples are already at precancerous stages, from the viewpoint of altered DNA methylation, despite the absence of any remarkable histological changes and the lack of association with chronic inflammation and persistent infection with viruses or other pathogenic microorganisms (17–20). (a) In fact, the logistic model adjusted by sex, age and experimental batch revealed that DNA methylation levels on 4830 probes were already altered in N samples compared with those in C samples (FDR, $q = 0.01$, Table I). (b) In order to reveal DNA methylation alterations inherited by clear cell RCCs themselves, ordered differences of DNA methylation level from C to N and then to T samples were examined by the cumulative logit model adjusted by sex, age and experimental batch. Ordered differences from C to N and then to T samples were observed on 11 089 probes (FDR, $q = 0.01$, Table I). (c) In order to reveal the cancer-prone DNA methylation alterations, differences in DNA methylation levels between 104 paired samples of N and T assayed in the same experimental batch were examined using the Wilcoxon matched pairs test. Significant differences between N and the corresponding clear cell RCCs themselves were observed on 10 870 probes (FDR, $q = 0.01$, Table I).

DNA hypermethylation frequently occurred at the very early stages of renal carcinogenesis [(a) in Table I], whereas DNA hypomethylation was also observed during progression to established cancers [(b) and (c) in Table I]. Eight hundred and one probes satisfied all of the above criteria (a)–(c) (Table I): DNA methylation alterations on these 801 probes (Supplementary Table S2, available at *Carcinogenesis* Online) were already evident in N samples, and were inherited by and strengthened in T samples.

Table I. DNA methylation alterations during renal carcinogenesis

The number of probes showing DNA hypermethylation and DNA hypomethylation	
(a) The probes on which DNA methylation levels were altered in samples of non-cancerous renal cortex tissue (N) obtained from patients with clear cell RCCs relative to those in samples of normal renal cortex tissue (C) obtained from patients without any primary renal tumor. (Logistic model adjusted by sex, age and experimental batch; FDR, $q = 0.01$.)	
DNA hypermethylation ($\beta_N > \beta_C$)	4589[a]
DNA hypomethylation ($\beta_N < \beta_C$)	241[b]
Total	4830
(b) The probes on which DNA methylation levels showed ordered differences from C to N, and then to tumorous tissue (T) samples. (Cumulative logit model adjusted by sex, age and experimental batch; FDR, $q = 0.01$.)	
DNA hypermethylation ($\beta_C < \beta_N < \beta_T$, $\beta_C < \beta_N \fallingdotseq \beta_T$ or $\beta_C \fallingdotseq \beta_N < \beta_T$)	6653
DNA hypomethylation ($\beta_C > \beta_N > \beta_T$, $\beta_C > \beta_N \fallingdotseq \beta_T$ or $\beta_C \fallingdotseq \beta_N > \beta_T$)	4436
Total	11 089
(c) The probes on which DNA methylation levels differed between T and the corresponding N samples (Wilcoxon matched pairs test; FDR, $q = 0.01$)	
DNA hypermethylation ($\Delta\beta_{T-N} > 0$)	5408
DNA hypomethylation ($\Delta\beta_{T-N} < 0$)	5462
Total	10 870

[a]Among the 4589 probes, 2675 showed DNA hypermethylation in T samples than in C samples ($\beta_T > \beta_C$; FDR, $q = 0.01$).

[b]Among the 241 probes, 126 showed DNA hypomethylation in T samples than in C samples ($\beta_T < \beta_C$; FDR, $q = 0.01$).